

Electron-impact-induced allowed transitions in Cs₂

A. Laricchiuta*

CNR IMIP Bari, via Amendola 122/D, 70126 Bari, Italy

G. Capitta

Department of Chemistry, University of Bari, Bari, Italy

R. Celiberto

Department of Water Engineering and Chemistry, Polytechnic of Bari, and CNR IMIP Bari, Bari, Italy

M. Capitelli

Department of Chemistry, University of Bari, and CNR IMIP Bari, Bari, Italy

(Received 18 March 2012; published 29 June 2012)

Allowed vibronic transitions to the two lowest singlet electronic terms induced by electron impact in the cesium dimer are theoretically investigated in the frame of the semiclassical impact parameter method. All relevant quantities characterizing the transitions, i.e., transition dipole moments, Franck-Condon factors, and vibronic moments, are derived and compared with results in the literature. Total and vibrationally resolved cross sections for excitations initiated from $v'' = 0-45$ vibrational levels of the ground electronic state are calculated and the role of vibrational excitation is discussed.

DOI: [10.1103/PhysRevA.85.062713](https://doi.org/10.1103/PhysRevA.85.062713)

PACS number(s): 34.80.Gs, 33.70.Ca, 52.20.-j

I. INTRODUCTION

Theoretical and experimental investigation of the Cs₂ dimer has been, in recent years, mainly oriented to the spectroscopic characterization of electronic states, due to their relevance in laser applications [1]. The optically allowed excitation to the first excited states $A^1\Sigma_u^+$ and $B^1\Pi_u$ have been studied, extracting the spectroscopic parameters [2,3] and the Franck-Condon factors for (v', v'') transitions [4-8]. The high-lying excited singlet states, $C^1\Sigma_u^+$ and $D^1\Pi_u$ have been investigated extensively [9,10], being the main components of the visible absorption spectrum of Cs₂, with vibrational progression strongly perturbed by spin-orbit interaction with triplet terms, and contributing to the atomic cesium budget through predissociation mechanisms [11-13].

However, the wide interest in cesium is also motivated in literature by the role played in modern negative ion sources for fusion applications [14-16], whose efficiency has been observed to be highly sensitive to the presence of atomic cesium at a low concentration. The mechanism is still not clear and is debated in the literature. In fact direct conversion at the cesiated surfaces of the reactor has been conjectured [17-19], though the role of gas-phase processes, governing the H⁻ formation in old volume sources, is to be considered [20]. Recently, in the development of accurate spectroscopic techniques (cavity ring-down spectroscopy) for the reliable estimation of H⁻ absolute volume density in rf-driven sources, a large enhancement of negative ion production in cesium-seeded operation has been shown, also measuring an additional adsorption in the afterglow of the discharge that has been attributed to the Cs₂ dimer [21].

Modeling of negative ion sources, assisting the designing phase, has shown that non-equilibrium conditions in plasma

systems are critically important, affecting the rate of production of negative hydrogen [22,23]. This consideration justifies the efforts made toward the inclusion of a detailed kinetics in the modeling of these devices, allowing the description of nonequilibrium features of internal distributions and the estimation of the role of excited species. The main requirement for state-to-state kinetics is state-specific dynamic information for elementary processes. Thus the derivation of a complete set of cross sections, with dependence on the internal quantum states of colliding species, could be considered the first step toward an accurate and realistic simulation. Attempts have been made to include cesium kinetics in the modeling of modern negative ion sources [15,24,25], but the poor knowledge of cross sections for elementary processes involving cesium represents the main obstacle. Theoretical investigation has focused on electron-impact-induced ionization and excitation of atomic cesium [26-28].

In the present work electron-impact-induced excitation processes in vibrationally excited Cs₂ molecules to the two lowest excited states, i.e.,



have been studied, in the frame of the semiclassical impact parameter method (IPM), with the perspective of creating a database for modeling and trying to remedy the lack of information in the literature on the dynamics of e -Cs₂ collisions.

II. METHOD OF CALCULATION

The IPM, in its original formulation for optically allowed transitions induced by electron impact [29,30], has been widely used in the calculation of state-to-state cross sections for a number of processes involving vibrationally excited diatomic molecules [30-33]. The basic idea of the method, which does

*annarita.laricchiuta@ba.imip.cnr.it

not include exchange [29], consists in a classical description of the incident electron motion (for which a straight-line trajectory is assumed), with the further constraint of the dominance of “distant collisions,” to avoid overlap effects with the molecular cloud, which would require a quantum description of the incident electron motion.

In this approach, the electron-target interaction potential, expressed in terms of classical trajectory, is a time-dependent function, and consequently, the collisional dynamics is also described by a time-dependent Schrödinger equation. The initial and final states of the molecular target are described fully quantum mechanically with respect to both electronic and nuclear motions.

The IPM provides an accuracy comparable with that of the Born approximation, to which it reduces at very high energies. In fact a better behavior of the cross section obtained in the IPM is observed for intermediate and lower energies with respect to the Born approximation, which overestimates the cross-section value as the incident energy decreases toward the threshold. Near the threshold, however, the IPM becomes less accurate and a quantum description of incident electron motion in this energy region becomes necessary.

Recalling briefly the main formulas, the state-to-state cross section $\sigma_{v'',v'}^{\alpha_i \rightarrow \alpha_f}(E)$ for an electron-impact-induced transition from the v'' vibrational level of the α_i electronic state to the v' vibrational level of the final α_f electronic state of a diatomic molecule is expressed as

$$\sigma_{v'',v'}^{\alpha_i \rightarrow \alpha_f}(E) = S_{v'',v'}^{\alpha_i, \alpha_f} D_{v'',v'}^{\alpha_i, \alpha_f}(E), \quad (2)$$

where E is the collision energy. The “structural factor” $S_{v'',v'}^{\alpha_i, \alpha_f}$, related to the quantum structure of the target, is defined by

$$S_{v'',v'}^{\alpha_i, \alpha_f} = \frac{m^2 e^2}{3g_i \hbar^4} (2 - \delta_{\Lambda_i, 0})(2 - \delta_{\Lambda_f, 0}) \left| \int_0^\infty dR \chi_{v'}^{\alpha_f}(R) M_{\Lambda_i, \Lambda_f}^{\alpha_i, \alpha_f}(R) \chi_{v''}^{\alpha_i}(R) \right|^2, \quad (3)$$

with m , e , \hbar , and g_i the mass and charge of the electron, Planck’s constant, and the degeneracy factor for the α_i state, respectively. $\chi_v^\alpha(R)$ is the vibrational wave function, which depends on the internuclear distance R , and $M_{\Lambda_i, \Lambda_f}^{\alpha_i, \alpha_f}(R)$ is the usual electronic transition dipole moment characterized by the quantum numbers of the projection of electronic angular momentum on the internuclear axis Λ_i and Λ_f .

The “dynamical factor,” describing the inelastic scattering effects on the motion of incident electron, is given by

$$D_{v'',v'}^{\alpha_i, \alpha_f} = \frac{2\pi \hbar^2}{m^2 u_i^2} \left\{ \gamma_i \left[K_0(\gamma_i) K_1(\gamma_i) - \frac{\pi^2}{4} S_0(\gamma_i) S_1(\gamma_i) \right] + \gamma_f \left[K_0(\gamma_f) K_1(\gamma_f) - \frac{\pi^2}{4} S_0(\gamma_f) S_1(\gamma_f) \right] + \gamma [K_0(\gamma_i) K_1(\gamma_f) + K_0(\gamma_f) K_1(\gamma_i)] + \gamma \frac{\pi^2}{4} [S_0(\gamma_i) S_1(\gamma_f) + S_0(\gamma_f) S_1(\gamma_i)] + \left(\frac{u_i^2 - u_f^2}{u_i^2 + u_f^2} \right) \left[\ln \left(\frac{\gamma_f}{\gamma_i} \right) + \frac{\pi}{2} \int_{\gamma_i}^{\gamma_f} S_0(\gamma) d\gamma \right] \right\}, \quad (4)$$

where K_i and S_i are the modified Bessel and Struve functions, respectively, and u_i and u_f are the initial and final electron velocities. Moreover,

$$\begin{aligned} \gamma_i &= \frac{\rho_{v'',v'}^0 |\Delta E_{v'',v'}^{\alpha_i, \alpha_f}|}{\hbar} \frac{1}{u_i}, \\ \gamma_f &= \frac{\rho_{v'',v'}^0 |\Delta E_{v'',v'}^{\alpha_i, \alpha_f}|}{\hbar} \frac{u_i}{u_f^2}, \\ \gamma &= \frac{\rho_{v'',v'}^0 |\Delta E_{v'',v'}^{\alpha_i, \alpha_f}|}{\hbar} \frac{2u_i}{u_i^2 + u_f^2}, \end{aligned} \quad (5)$$

where $\Delta E_{v_i, v_f}^{\alpha_i, \alpha_f} = \epsilon_{v_f}^{\alpha_f} - \epsilon_{v_i}^{\alpha_i}$ is the transition energy, with ϵ_v^α the energy eigenvalue of the v vibrational level of the α electronic state. $\rho_{v'',v'}^0$ is a cutoff parameter introduced in the IPM to avoid divergent cross sections, whose value is set by equating the impact parameter and Born approximation cross sections at high energies.

The dissociative cross section $\sigma_{v''}^{\alpha_i \rightarrow \alpha_f}(E)$ is defined by the integral

$$\sigma_{v''}^{\alpha_i \rightarrow \alpha_f}(E) = \int_{\epsilon_{\text{th}}}^{\epsilon_{\text{max}}} \frac{d\sigma_{v'',\epsilon}^{\alpha_i \rightarrow \alpha_f}(E)}{d\epsilon} d\epsilon, \quad (6)$$

where $\sigma_{v'',\epsilon}^{\alpha_i \rightarrow \alpha_f}(E)$ is readily obtained from Eq. (2) by simply replacing the final quantum number v' with the continuum energy ϵ . The integration on the continuum spans from ϵ_{th} , i.e., the dissociation threshold for the excited electronic state, to $\epsilon_{\text{max}} = E + \epsilon_{v''}^{\alpha_i}$. The *total cross section* results from bound-bound and dissociative contributions.

One last remark is about the arising, in the original formulation, of a low-energy peak [34] due to the behavior of one term in the dynamical factor, i.e., $u_i^{-2} \gamma \frac{\pi^2}{4} S_0(\gamma_i) [S_1(\gamma_f) + S_0(\gamma_f) S_1(\gamma_i)]$. This term has a first derivative that becomes negative in the region close to the threshold. In the present paper a constant extrapolation has been applied to this term as E tends to the threshold value, thus producing an automatic smoothing.

III. COMPUTATIONAL DETAILS

A. Potential energy curves

Due to the high sensitivity of the Cs_2 system, potential energy curves as accurate as possible have been used for vibrational level calculation. For the ground state $X^1\Sigma_g^+$ (Fig. 1), in the region of the well, the Rydberg-Klein-Rees (RKR) potential of Amiot and Dulieu [35] was used, derived from the analysis of vibronic molecular spectra of Cs_2 and in excellent agreement with older results of Raab *et al.* [11]. The long-range part of the curve, correlating with the most accurate experimental value for the dissociation limit $D_e = 3649.84 \text{ cm}^{-1}$, has been described through the Morse/long-range model expansion with additional parameters [36]. The short-range repulsive branch of the potential has been extrapolated for $R < 6.6023$ bohr, by using the physically sound exponentially decreasing function, i.e., $V(R) = \alpha \exp(\beta R)$, whose parameter values $\alpha = 18.9498$ a.u. and $\beta = -1.0672 a_0^{-1}$ have been optimized through a best-fit procedure, to ensure a smooth connection with the potential energy values corresponding to the lowest R values in the RKR potential. Vibrational

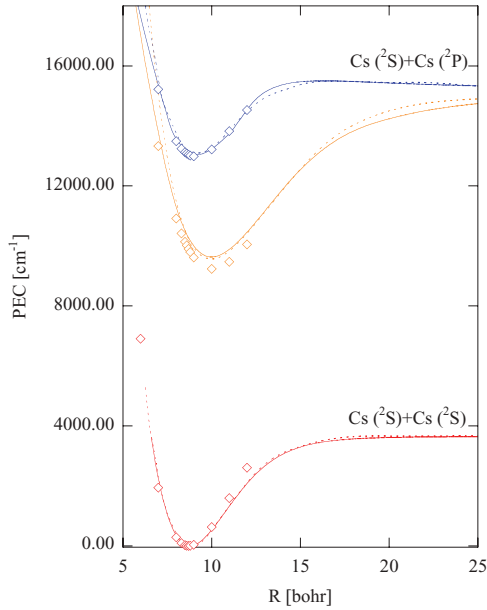


FIG. 1. (Color online) Potential energy curves of the ground state $X\ ^1\Sigma_g^+$ and the two lowest excited states $A\ ^1\Sigma_u^+$ and $B\ ^1\Pi_u$ of the Cs_2 molecule. Solid lines, reconstructed from RKR potentials in the literature; dotted lines, from Ref. [37]; symbols, *ab initio* results of this work.

ingenvalues ($\nu''_{\max} = 134$) for the ground-state $X\ ^1\Sigma_g^+$ of the Cs_2 dimer, obtained by direct numerical integration of the constructed potential in the radial Schrödinger equation, reproduce excellently the levels in the literature [35].

An analogous procedure has been adopted for the potential energy curves of the two excited states, correlating with $\text{Cs}(^2S) + \text{Cs}(^2P)$. The accurate value of the dissociation limit has been derived by adding to the molecular ground-state dissociation limit, $\text{Cs}(^2S) + \text{Cs}(^2S)$, the energy for the excitation of atomic cesium to the (2P) state, averaging in the statistical weight the two sublevels, ($^2P_{1/2}$) and ($^2P_{3/2}$), leading to the value $11\ 547.627\ \text{cm}^{-1}$, which is in excellent agreement with the experimental value reported in Ref. [38]. For the $A\ ^1\Sigma_u^+$ state no extended RKR potential is available, therefore reference is made to theoretical *ab initio* results of Krauss [39], however, data have been shifted so as to fit the experimental $R_{\text{eq}}^{\text{exp}} = 10.00\ \text{bohr}$ ($T_e^{\text{exp}} = 9627.06\ \text{cm}^{-1}$ [4] is close to the value of $T_e^{\text{theo}} = 9620\ \text{cm}^{-1}$ [39] from theory). The short-range exponentially decreasing extrapolation function has been adopted for $R \leq 5\ \text{bohr}$, with parameters $\alpha = 0.27484\ \text{a.u.}$ and $\beta = -0.2108\ a_0^{-1}$, while for $R > 20\ \text{bohr}$ the usual asymptotic inverse power expansion, including terms due to electrostatic interaction and dispersion forces, has been considered:

$$V(R) = D_e + \frac{C_3}{R^3} + \frac{C_6}{R^6} + \frac{C_8}{R^8}. \quad (7)$$

The $C_6 = -26\ 087\ \text{hartree}\ a_0^{-6}$ and $C_8 = -6\ 416\ 535\ \text{hartree}\ a_0^{-8}$ values have been taken from Ref. [40], while the C_3 coefficient has been set to $30.0\ \text{hartree}\ a_0^{-3}$ with respect to the theoretically predicted value of $24.27\ \text{hartree}\ a_0^{-3}$, to smoothly connect with theoretical *ab initio* results.

TABLE I. Vibrational eigenvalues (from the minimum of the A state) of the excited state $A\ ^1\Sigma_u^+$ of Cs_2 compared with the literature [4].

ν'	$\epsilon_{\nu'} [4]\ (\text{cm}^{-1})$	$\epsilon_{\nu'}\ (\text{cm}^{-1})$
0	18.185	20.624
1	54.915	53.993
2	92.327	87.269
3	130.33	120.45
4	168.85	153.51
5	207.79	186.47
6	247.10	219.30
7	286.70	252.01
8	326.53	284.60
9	366.54	317.06

In Table I a comparison is shown of the first few vibrational eigenvalues, of the large number of levels ($\nu'_{\max} = 347$) sustained by the excited state $A\ ^1\Sigma_u^+$ ($\nu' = 0-9$) with results from fluorescence spectroscopy of Verges and Amiot [4]. The fundamental level is satisfactorily reproduced, however, for higher vibrational levels deviations, in any case below 16%, are observed that could be ascribed to the shape of the potential energy curve of the excited term.

The $B\ ^1\Pi_u$ potential energy curve has been constructed starting from the RKR data in Ref. [8] for R values in the interval $7.87-10.94\ \text{bohr}$. As before, the region of small internuclear distances has been described through the exponential decay function ($\alpha = 0.18453\ \text{a.u.}$, $\beta = -0.13856\ a_0^{-1}$), while the curve to the dissociation limit through Eq. (7) with coefficients $C_3 = 10.87\ \text{hartree}\ a_0^{-3}$, $C_6 = -13\ 210\ \text{hartree}\ a_0^{-6}$, and $C_8 = -2.078 \times 10^6\ \text{hartree}\ a_0^{-8}$ [40,41].

Seventy bound vibrational levels ($\nu'_{\max} = 69$) are sustained by this potential energy curve. It is interesting to note the special feature affecting the long-range portion of the B -state potential (see Fig. 1), which exhibits a barrier of $\sim 302\ \text{cm}^{-1}$ above the dissociation limit, located at $R = 16.2$, $a_0 = 8.6\ \text{\AA}$, determined by the repulsive positive C_3/R^3 term in the long-range expansion [Eq. (7)], in satisfactory accord with theoretical results of Jeung *et al.* [42], locating the barrier at $R \approx 8\ \text{\AA}$, with a rise of $250\ \text{cm}^{-1}$ above D_e . The presence of this maximum causes the existence of 18 *quasibound* vibrational levels, i.e., levels with energy above the dissociation threshold, characterized by the probability of tunneling the energy barrier leading to dissociation. These levels are resonances in the scattering dynamics in cesium atom collisions, corresponding to the physical occurrence of trapped atoms in the molecular system. The numerical module handling the vibrational structure of electronic states, included in the impact parameter code, is able to estimate the position and the energy width (Γ) of these resonances in the frame of the *internal amplitude method* [34]. The width of the resonance Γ , related to the surviving time of the quasibound state against tunneling ($\tau = \hbar/\Gamma$), except for the last four levels, lying very close to the barrier top, is so small that these levels can be regarded as bound.

B. *Ab initio* calculations of transition dipole moments

Electronic structure calculations, at the MRCI level including singly and doubly excited configurations, have been performed with the GAMESS package [43] for electronic term energies and transition dipole moments, in allowed transitions under consideration, neglecting spin-orbit and relativistic effects. Core electrons have been described by means of an *effective core potential* (ECP) [44], leading to a reduced 18-electron dimer system. The adopted basis set is a triple- ζ ($7s,6p,3d$) contracted to ($5s,3p,3d$) [45] with eight virtual orbitals in the active space. Molecular geometries in the interval 6.0 – $12.0 a_0$ of R have been considered. In Fig. 1 *ab initio* energies for the three electronic states under investigation have also been reported and compared with reconstructed potential energy curves and *ab-initio* results in literature [37], showing a good agreement in the potential well region, the equilibrium internuclear distance values for the three states being well reproduced ($R_{\text{eq}}^X = 8.7$ bohr, $R_{\text{eq}}^A = 10.0$ bohr, and $R_{\text{eq}}^B = 9.0$ bohr, compared to 8.74, 10.11, and 9.23 bohr from Ref. [39], respectively). Upon increasing the nuclei separation ($R > 12.0 a_0$), some discrepancies arise, probably due to a deficiency in the active space; in fact the dominant configuration-state functions, ensuring a correct estimation of the correlation energy for the electronic terms, change with the internuclear separation and the ground-state dissociation energy is not accurately reproduced.

The behavior of the transition dipole moment, reported in Fig. 2 for the two excitations, shows a weak monotonic increase with the internuclear coordinate. Transitions initiated from excited vibrational levels are expected to be slightly

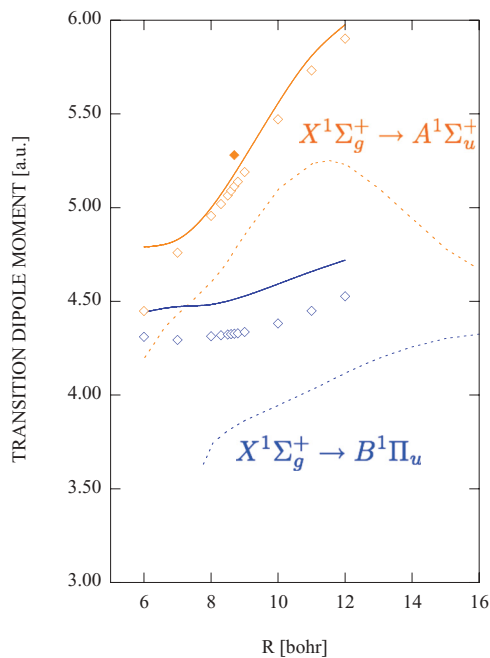


FIG. 2. (Color online) Transition dipole moment for transition to the $A^1\Sigma_u^+$ and $B^1\Pi_u$ states in Cs_2 . Open diamonds, *ab initio* results from this work; dotted lines, *ab initio* results of Ref. [37]; solid lines, phenomenological approach [46]; filled diamond, value for the $X \rightarrow A$ transition derived by Smirnov [5] from an analysis of vibronic spectra.

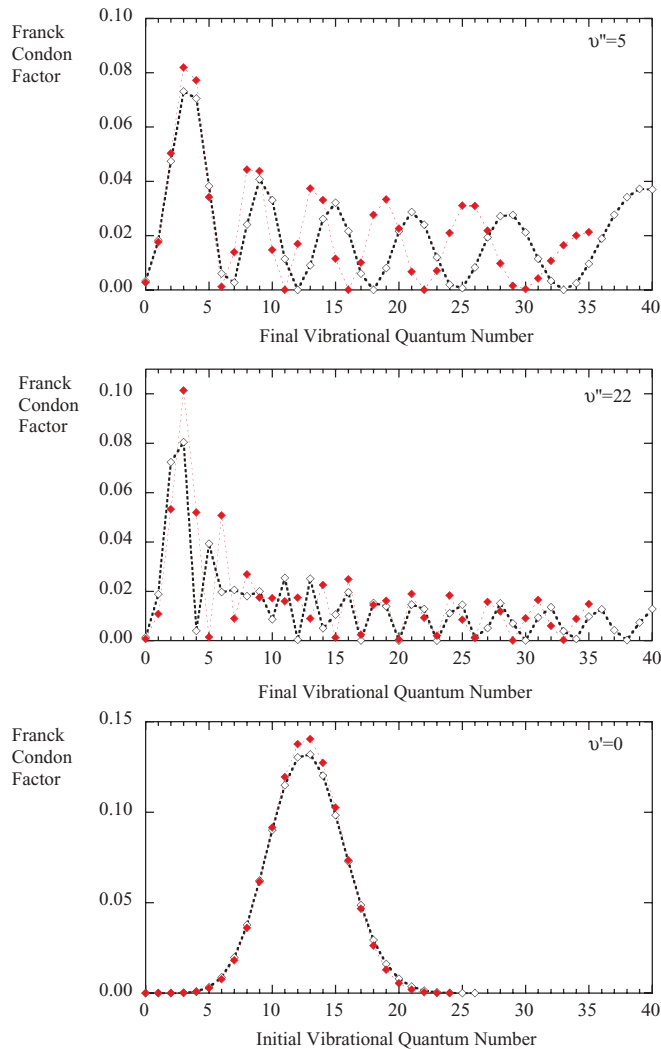


FIG. 3. (Color online) Frank-Condon factors, for the $X^1\Sigma_g^+ \rightarrow A^1\Sigma_u^+$ transition in Cs_2 , for selected initial or final vibrational levels. Open symbols, present results; filled symbols, results from Refs. [6,7].

favored; in fact, considering *vertical transitions*, these levels are characterized by the value of the transition dipole moment corresponding to the outer classical turning point, progressively moving to the region of higher R values.

The R dependence of transition dipole moments for the considered transitions have been published in very recent papers [37,47], where also the spin-orbit coupling with the triplet term $b^3\Pi_u$ is taken into account. In Ref. [47] *ab initio* calculations have been performed with the MOLPRO code, including dynamical correlation effects by the internally contracted multireference configuration interaction method (MRCI), the complete active space (CAS) consisting of the $7\sigma_{g,u}$, $4\pi_{g,u}$, and $2\delta_{g,u}$ optimized molecular orbitals. The ℓ -independent core-polarization potentials have been used, implicitly accounting for core-polarization effects, with explicit treatment only of the two valence electrons in the MRCI. In the present *ab initio* calculation no core polarization potentials are included, not being available for the GAMESS code, and the core polarization has been included considering four active electrons in the CAS, generating the reference configuration-state functions. Core-polarization effects act to

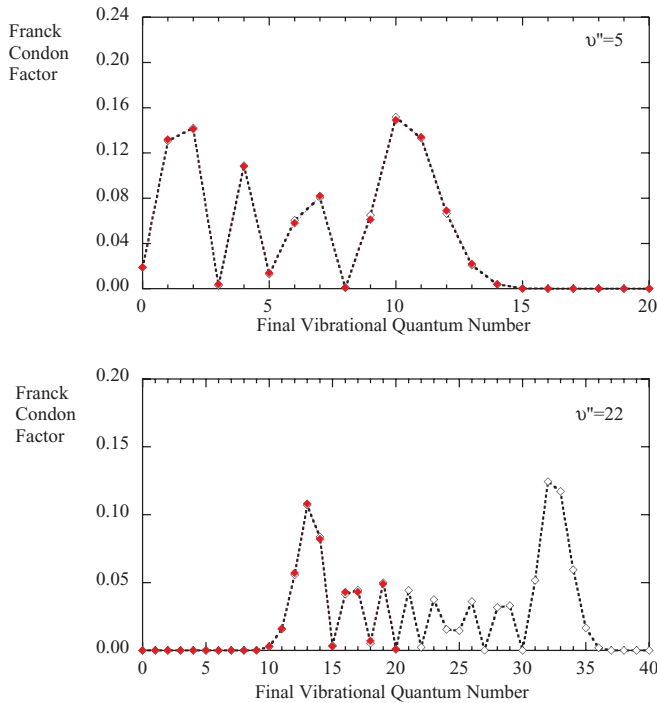


FIG. 4. (Color online) Franck-Condon factors, for the $X\ ^1\Sigma_g^+ \rightarrow B\ ^1\Pi_u$ transition in Cs_2 , as a function of the final vibrational quantum number v' for selected initial vibrational levels, v'' . Open symbols, present results; filled symbols, results from Ref. [8].

shorten the bond length and thus attain the experimental value for the R_{eq} of electronic states [42].

Despite the satisfactory accord of the potential energy curves (see Fig. 1), only a semiquantitative agreement is found for transition moments (see Fig. 2). The monotonic increasing behavior for R in the interval 6–11 a_0 is confirmed, however, with lower absolute values in Refs. [37,47], leading to discrepancies of around 7% and 15% for the $X \rightarrow A$ and $X \rightarrow B$ transitions, respectively. The impact on the corresponding IPM excitation cross sections could be roughly estimated considering vertical excitations and the propagation of differences in the structural factor, S^{α_i, α_f} being proportional to the square modulus of the transition dipole moment at the classical turning point and thus lowering the cross-section values of approximately 15% and 30%, respectively.

It should be pointed out that the present results are predictively reproduced using a phenomenological approach proposed by Woerdman [46], assuming a value for the oscillator strength for transition ($6s \rightarrow 6p$) in atomic cesium equal to 1.21 [48]. The approach has been validated for the dimers of elements in the first group of the periodic table, finding a close agreement with *ab initio* methods for Li_2 and Na_2 . In Fig. 2 the value for the $X \rightarrow A$ transition, derived by Smirnov [5] from the experimental determination of the electron transition strength in the interval $R = 0.454\text{--}0.475\text{ nm} = 8.579\text{--}8.976\text{ }a_0 \sim R_{\text{eq}}^X$ is also reported.

C. Vibrational analysis

A ($v'-v''$) matrix for $v'' = 0\text{--}45$ for Franck-Condon factors has been derived for the $\text{Cs}_2(X \rightarrow A)$ and ($X \rightarrow B$) transitions. Also, the contribution coming from the vibra-

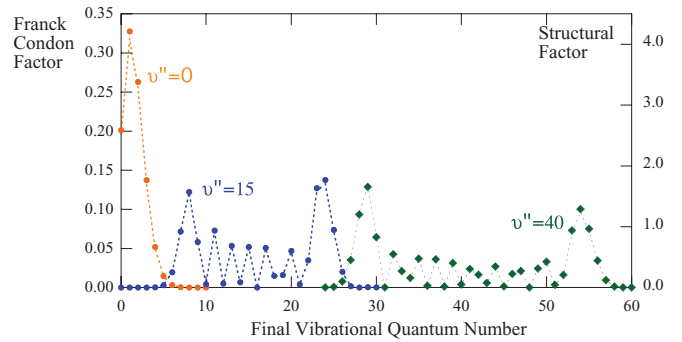


FIG. 5. (Color online) Symbols represent Franck-Condon factors (left axis) and dotted lines represent structural factors (right axis) as a function of the final vibrational quantum number, v' , of the excited state for selected values of the initial vibrational quantum number, v'' , of the ground state, in the $\text{Cs}_2\ X\ ^1\Sigma_g^+ \rightarrow B\ ^1\Pi_u$ transition.

tional continuum has been considered, estimating the Franck-Condon densities, corresponding to the integration of the vibrational overlap in the continuum. In the limit of completeness of the vibrational ladder of the excited state, the sum of the Franck-Condon factors and density should approach 1, due to the closure relation. The overlap of the ground-state vibrational levels with the continuum is found to be small, leading to the general conclusion that, in the considered transition, the vibronic excitation is the dominant process, while dissociative channels are not favored and are therefore neglected. In Fig. 3 Franck-Condon factors have been compared with those in Refs. [6,7]. Except for the first few levels, increasing the final vibrational quantum number corresponds to a dephasing of the two series of data, with a shift of the predicted maxima to higher values of v' . A better agreement is found for $v' = 0$, giving a strong indication of the sensitivity of this system to the relative position and shape of the potential energy curves for the two electronic terms.

For the $X\ ^1\Sigma_g^+ \rightarrow B\ ^1\Pi_u$ transition a comparison with results in Ref. [8] is displayed in Fig. 4. Actually the Franck-Condon factors in the literature refer to the rotationally excited Cs_2 dimer, in particular, the Q branch, i.e., $\Delta j = 0$, transitions with $j = 50$, while the results obtained in the present work assume a rotationless dimer, i.e., $j = 0$. For low-lying vibrational levels, i.e., for $v'' = 5$ and 22, the rotational perturbation seems not to be effective, resulting in an excellent agreement of Franck-Condon factors, as is appreciable in Fig. 4.

Structural factors follow closely the position and relative intensity of maxima in the profile of corresponding Franck-Condon factors (see Fig. 5), due to the smooth R dependence of the transition dipole moment. Therefore they could give an indication of the favored vibronic transitions and, in turn, the state-resolved cross-section dependence on the initial and final vibrational quantum numbers.

IV. RESULTS

A. Born cross sections

The *cutoff parameters*, ρ_0 , are energy-independent parameters whose values are chosen so as to ensure the correct high-energy behavior of the IPM cross section, avoiding the

divergence of the probability. In the computational procedure the cross section is required to coincide with the value obtained in a different approximation, accurate at high collision energies, i.e., the Born approximation. Born cross sections have been obtained from the *ab initio* MRCI wave functions of electronic states α_i and α_f ,

$$(\sigma_{\nu''}^{\alpha_i, \alpha_f})^B(E) = \langle \nu'' | \frac{4\pi m e^4}{\hbar^2 k^2 \Delta E_{\alpha_i, \alpha_f}} \int_{|k-k'|}^{k+k'} dK \frac{\mathcal{F}_{\alpha_i, \alpha_f}^B(K)}{K} | \nu'' \rangle, \quad (8)$$

with K the momentum transferred in the collision and \mathcal{F} the *generalized oscillator strength* for the electronic transition, i.e.,

$$\mathcal{F}^B(K) = \frac{2m}{\hbar^2 K^2} \Delta E_{\alpha_i, \alpha_f}(R) \int \frac{d\hat{R}}{4\pi} \left| \langle \alpha_f | \sum_j e^{i(K \cdot r_j)} | \alpha_i \rangle \right|^2. \quad (9)$$

The number of levels is limited by the interval of inter-nuclear distances explored in the *ab initio* step; in fact, the convergence of the integral in Eq. (8) forces constraints on the integration limits compatible with the region of R values where the probability of the vibrational wave function is different from 0. Highly excited vibrational states are usually characterized by a maximum of probability in proximity to the external classical turning point that gives the dominant contribution to the integral in Eq. (8) and that is progressively shifted in the region of high R values, which requires the corresponding value of $\sigma^{\alpha_i, \alpha_f}(E, R)$. The number of levels actually considered for Cs_2 is $\nu'' = 45$. The vibrationally resolved values for total cross sections in the Born method and the IPM have been required to coincide at $E = 1000$ eV. The vibrational profile, displayed in Fig. 6, exhibits for both transitions a monotonic increasing character in the explored range, reflecting the behavior of transition dipole moments. The

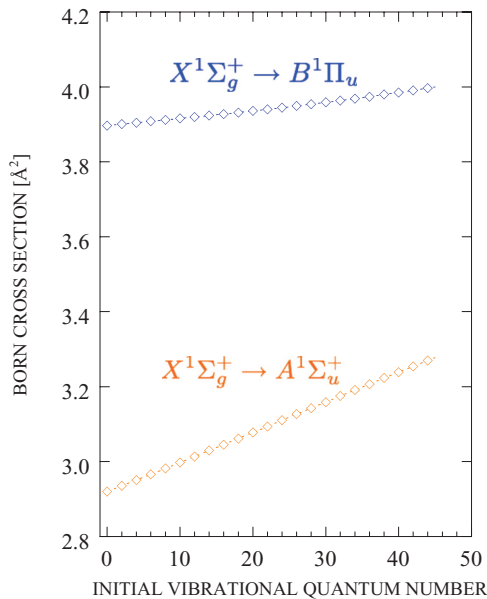


FIG. 6. (Color online) Born cross sections as a function of the initial vibrational quantum number at $E = 1000$ eV, for allowed transitions from the ground state $X^1\Sigma_g^+$ to the $A^1\Sigma_u^+$ and $B^1\Pi_u$ excited states of the Cs_2 molecule.

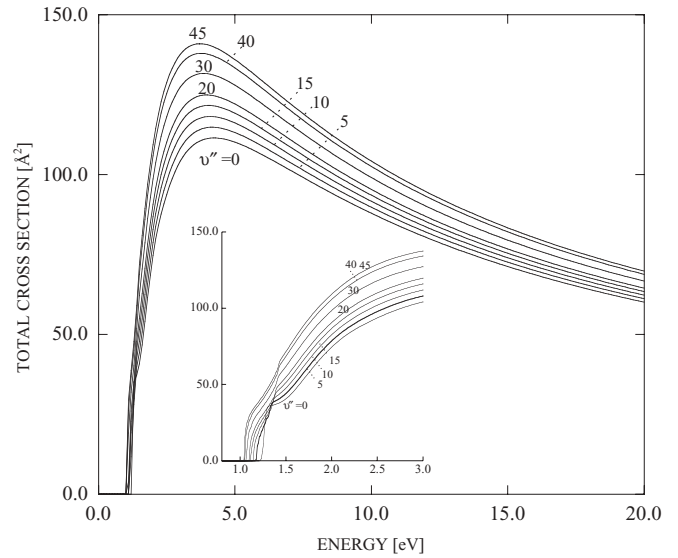


FIG. 7. Total cross sections for the electron-impact excitation of Cs_2 , in the transition $X^1\Sigma_g^+ \rightarrow A^1\Sigma_u^+$, as a function of the collision energy, for different initial vibrational levels. Inset: Magnification of the threshold region.

dependence on ν'' is actually weak, with quite high absolute values, depicting a very favorable transition not significantly affected by the vibrational excitation of the target molecule.

B. IPM total cross sections

The total cross sections for the process $X^1\Sigma_g^+ \rightarrow A^1\Sigma_u^+$ are shown in Fig. 7 as a function of the incident energy. Each curve is labeled by the value of the initial quantum number ν'' , varying in the interval 0–45.

The first aspect to be pointed out is that the absolute value of cross section is quite high, with a maximum of

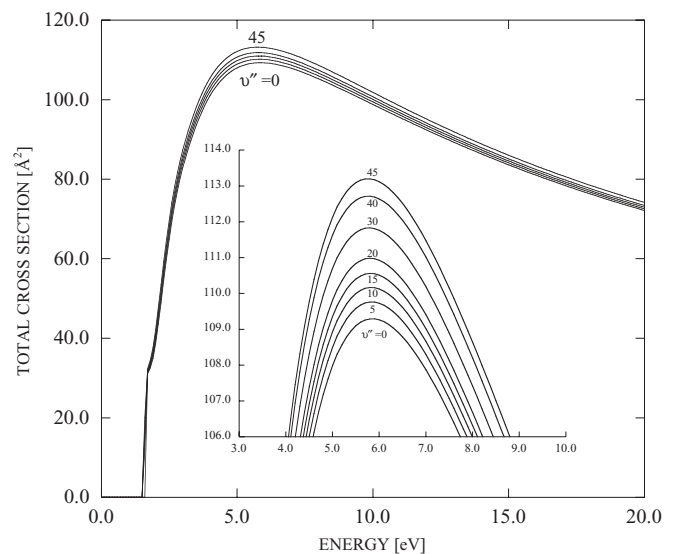


FIG. 8. Total cross sections for electron-impact excitation of Cs_2 , in the transition $X^1\Sigma_g^+ \rightarrow B^1\Pi_u$, as a function of the collision energy, for different initial vibrational levels. Inset: Magnification of the peak region.

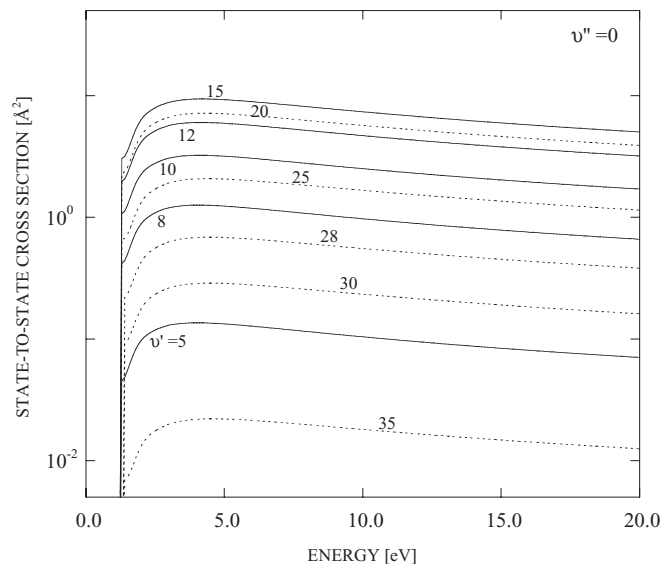


FIG. 9. State-to-state cross sections for electron-impact vibronic excitation of Cs_2 , in the transition $X^1\Sigma_g^+ \rightarrow A^1\Sigma_u^+$, as a function of the collision energy, for a selected initial vibrational level $v'' = 0$ and different final vibrational levels v' .

100 \AA^2 at low electron energies, localized at approximately 5 eV, thus showing the high probability of this process. The excitation does not result in dissociation, the overlap with the discrete levels of the excited states being extremely favored for the $X^1\Sigma_g^+ \rightarrow A^1\Sigma_u^+$ transition. As expected, the initial vibrational excitation produces a shift of the threshold to lower energies, correlated with the lowering of the transition gap and with the corresponding shift of the cross-section peaks. Actually, as in the Born cross section, the vibrational energy content of the target Cs_2 dimer does not affect the cross section strongly, though a monotonic increase with v'' is observed. The

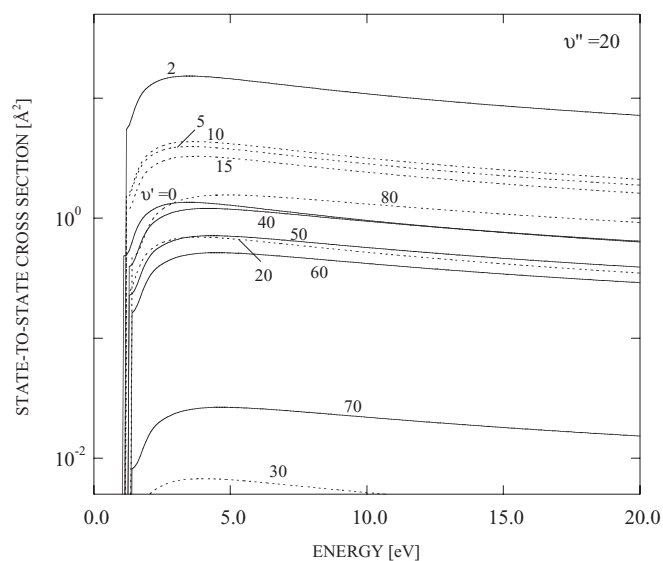


FIG. 10. State-to-state cross sections for electron-impact vibronic excitation of Cs_2 , in the transition $X^1\Sigma_g^+ \rightarrow A^1\Sigma_u^+$, as a function of the collision energy, for a selected initial vibrational level $v'' = 20$ and different final vibrational levels v' .

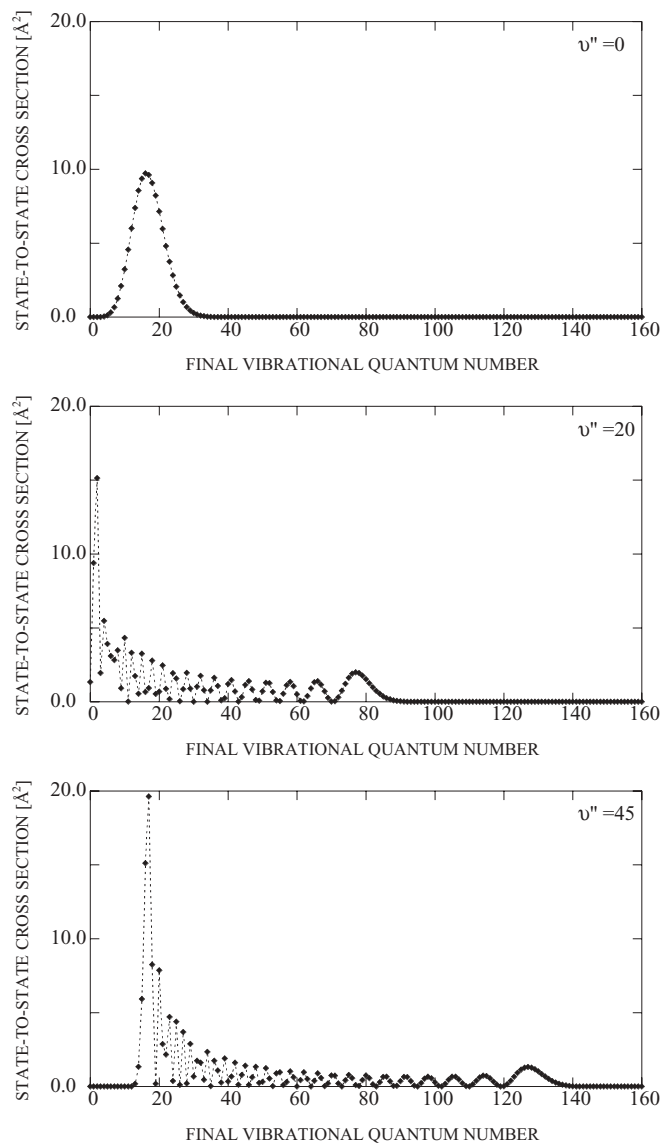


FIG. 11. State-to-state cross sections for electron-impact vibronic excitation of Cs_2 , in the transition $X^1\Sigma_g^+ \rightarrow A^1\Sigma_u^+$, as a function of the final vibrational quantum number, v' , for different initial vibrational quantum numbers, v'' , at collision energies $E = 4.0 \text{ eV}$.

vibrational profile is governed by the structural factor summed over the final vibrational ladder and, thus, almost unchanged with collision energy.

The same considerations can be applied to the $X^1\Sigma_g^+ \rightarrow B^1\Pi_u$ transition, displayed in Fig. 8 for selected initial vibrational levels, with a vibrational dependence even weaker than in the previous case, requiring a magnification of the peak region.

C. IPM state-to-state cross sections

In the case of *state-to-state* cross sections a huge number of data have been derived, [50] which need careful analysis for the outline of general trends, the dynamical quantity, $\sigma_{v'',v'}(E)$,

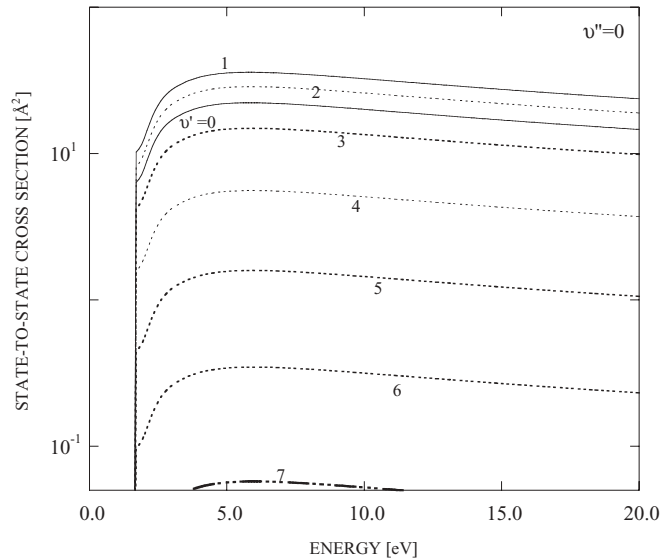


FIG. 12. State-to-state cross sections for electron-impact vibronic excitation of Cs_2 , in the transition $X^1\Sigma_g^+ \rightarrow B^1\Pi_u$, as a function of the collision energy, for a selected initial vibrational level $v'' = 0$ and different final vibrational levels v' .

being dependent on the initial and final vibrational quantum number and on the collision energy; therefore different groups of results are considered, restricted to energy or vibrational profiles.

In Figs. 9 and 10 the state-specific cross sections for $X \rightarrow A$ vibronic excitation in Cs_2 are reported for selected values of the initial and final vibrational levels. In this case a large effect is connected to the vibrational excitation of the target; in fact the corresponding cross sections need a logarithmic scale to be simultaneously displayed. The energy profile follows the expected behavior, with a sharp rise at threshold, a maximum, and a smooth monotonic decrease to the high-energy value. The chosen representation allows us to appreciate that, except for the absolute value, the cross sections have a shape with the collision energy that is essentially unaffected by the vibrational levels involved in the vibronic transition. This observation confirms a substantial insensitivity of the vibrational profile of the energy, except in the threshold region. The large and irregular variation of the cross-section value with the initial vibrational quantum number is modulated by the oscillatory behavior of the structural factor. The energy separation of electronic terms actually being small, the thresholds of these processes are localized in a narrow region of low-energy values. Once v'' is selected the increase in v' produces a shift in the threshold energy, reflecting a higher value of the transition energy.

In Fig. 11, the corresponding vibrational profiles are displayed at a fixed value of the collision energy, selected to be close to the cross-section maximum. Moreover, increasing from $v'' = 0$ to 45, the profile changes markedly from the usual bell shape for the fundamental level to irregular oscillatory features. It is interesting to note that the high-energy part of the excited vibrational ladder is efficiently populated only by transitions from the high-lying vibrational levels of the ground state, thus in the present work, limited to $v'' = 0-45$, only

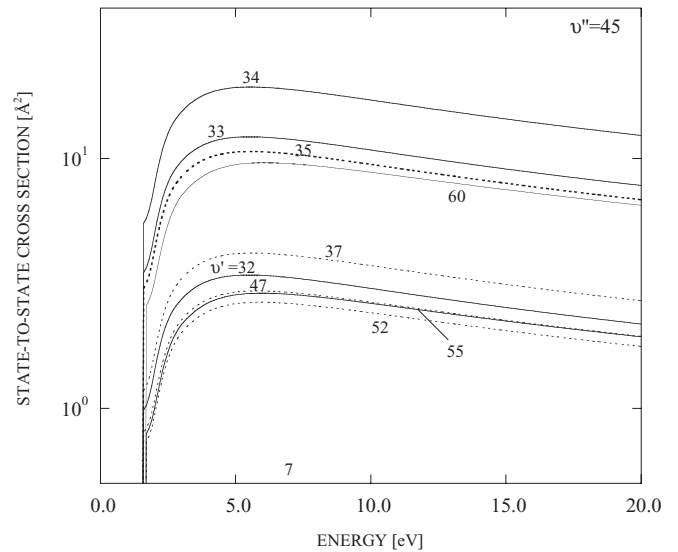


FIG. 13. State-to-state cross sections for electron-impact vibronic excitation of Cs_2 , in the transition $X^1\Sigma_g^+ \rightarrow B^1\Pi_u$, as a function of the collision energy, for a selected initial vibrational level $v'' = 45$ and different final vibrational levels v' .

levels up to $v' = 140$ of the 348 are actually involved in the excitation process.

The state-to-state cross sections for the $X^1\Sigma_g^+ \rightarrow B^1\Pi_u$ transition are reported in Figs. 12 and 13 for selected initial vibrational levels $v'' = 0$ and 45. The final vibrational levels were chosen from among those having a higher contribution to the total cross section. As in the case of the $X \rightarrow A$ transition the vibrational excitation of the target molecule promotes significant excitation to higher levels of the excited state.

V. CONCLUSIONS

Total and state-to-state cross sections for vibronic transitions to the two lowest excited states, $A^1\Sigma_u^+$ and $B^1\Pi_u$, induced by electron impact on Cs_2 have been calculated in the frame of the IPM, with the perspective of establishing detailed dynamic information for kinetic models of nonequilibrium plasmas containing cesium. Analysis of the results, following a critical comparison of the *ab initio* data with results in the literature, showed clearly that the excitation processes under investigation are strongly favored, with high absolute values of the cross section. The vibrational dependence of the total cross sections, in both transitions, is weak, with a small enhancement with the vibrational excitation of the target, reflecting the almost-constant behavior of the transition dipole moment with the internuclear distance. On the contrary, a large effect is observed in state-to-state cross sections, modulated by the overlapping of vibrational wave functions coupled in the excitation transition. The contribution of excitations leading to dissociation is negligible, the initial vibrational levels considered in this work being effectively coupled only to the discrete vibrational ladder of the excited states.

Assessment of the accuracy of the present results would require a comparison with experimental cross sections or with other theoretical results obtained in the frame of different

approaches, not available for this system. Uncertainties within 15%–30% could arise in the evaluation of the dipole transition strength. General considerations regarding the accuracy of the IPM are expected to be valid, i.e., the IPM is a first-order theory, giving a reliable high-energy estimation of the cross section and improving the Born approximation results in the low-energy region. The results obtained for different molecular

targets (H_2 , O_2) [32,33,49] have demonstrated a satisfactory agreement with more sophisticated theoretical approaches, while, in general, theoretical values overestimate experiments by a factor of 2.

Future research activity should focus on high-lying electronic terms of the cesium dimer, accounting for both dissociation and predissociation mechanisms.

-
- [1] M. Terrell and M. F. Masters, *Am. J. Phys.* **64**, 1116 (1996).
- [2] A. D. Smirnov, *Opt. Spectrosc.* **102**, 18 (2007).
- [3] A. L. Oldenburg, P. C. John, and J. G. Eden, *J. Chem. Phys.* **113**, 11009 (2000).
- [4] J. Verges and C. Amiot, *J. Mol. Spectrosc.* **126**, 393 (1987).
- [5] A. D. Smirnov, *J. Appl. Spectrosc.* **59**, 837 (1993).
- [6] A. D. Smirnov, *Mol. Spectrosc.* **78**, 553 (1995).
- [7] A. D. Smirnov, *J. Appl. Spectrosc.* **77**, 609 (2010).
- [8] U. Diemer, R. Duchowicz, M. Ertel, E. Mehdizadeh, and W. Demtröder, *Chem. Phys. Lett.* **164**, 419 (1989).
- [9] C. Amiot, W. Demtröder, and C. R. Vidal, *J. Chem. Phys.* **88**, 5265 (1988).
- [10] S. Kasahara, K. Otsuka, M. Baba, and H. Katô, *J. Chem. Phys.* **109**, 3393 (1998).
- [11] M. Raab, G. Höning, W. Demtröder, and C. R. Vidal, *J. Chem. Phys.* **76**, 4370 (1982).
- [12] S. Kasahara, Y. Hasui, K. Otsuka, M. Baba, W. Demtröder, and H. Katô, *J. Chem. Phys.* **106**, 4869 (1997).
- [13] Y. Kimura, H. Lefebvre-Brion, S. Kasahara, H. Katô, M. Baba, and R. Lefebvre, *J. Chem. Phys.* **113**, 8637 (2000).
- [14] M. Capitelli, M. Cacciatore, R. Celiberto, O. D. Pascale, P. Diomede, F. Esposito, A. Gicquel, C. Gorse, K. Hassouni, A. Laricchiuta *et al.*, *Nucl. Fusion* **46**, S260 (2006).
- [15] O. Fukumasa and R. Nishida, *Nucl. Fusion* **46**, S275 (2006).
- [16] A. J. T. Holmes and E. Surrey, *Plasma Sources Sci. Technol.* **2**, 235 (1993).
- [17] R. Trainham, C. Jacquot, D. Riz, A. Simonin, K. Miyamoto, Y. Fujiwara, and Y. Okumura, *Rev. Sci. Instrum.* **69**, 926 (1998).
- [18] M. Nishiura, M. Sasao, and M. Wada, *AIP Conf. Proc.* **639**, 21 (2002).
- [19] J. Sjakste, A. G. Borisov, and J. P. Gauyacq, *Nucl. Instrum. Methods Phys. Res. Sec. B* **230**, 323 (2005).
- [20] M. Capitelli and C. Gorse, *IEEE Trans. Plasma Sci.* **33**, 1832 (2005).
- [21] M. Berger, U. Fantz, S. Christ-Koch, and N. Team, *Plasma Sources Sci. Technol.* **18**, 025004 (2009).
- [22] C. Gorse, M. Capitelli, M. Bacal, J. Bretagne, and A. Laganá, *Chem. Phys.* **117**, 177 (1987).
- [23] K. Hassouni, A. Gicquel, and M. Capitelli, *Chem. Phys. Lett.* **290**, 502 (1998).
- [24] D. Pagano, C. Gorse, and M. Capitelli, *IEEE Trans. Plasma Sci.* **35**, 1247 (2007).
- [25] P. Diomede and S. Longo, *Plasma Sources Sci. Technol.* **19**, 015019 (2010).
- [26] M. Lukomski, J. A. MacAskill, D. P. Secombe, C. McGrath, S. Sutton, J. Teeuwen, W. Kedzierski, T. J. Reddish, J. W. McConkey, and W. A. van Wijngaarden, *J. Phys. B* **38**, 3535 (2005).
- [27] V. Zeman, R. P. McEachran, and A. D. Stauffer, *J. Phys. B* **27**, 3175 (1994).
- [28] V. Zeman, R. P. McEachran, and A. D. Stauffer, *J. Phys. B* **28**, 1835 (1995).
- [29] A. U. Hazi, *Phys. Rev. A* **23**, 2232 (1981).
- [30] M. J. Redmon, B. C. Garrett, L. T. Redmon, and C. W. McCurdy, *Phys. Rev. A* **32**, 3354 (1985).
- [31] R. Celiberto, M. Capitelli, N. Durante, and U. T. Lamanna, *Phys. Rev. A* **54**, 432 (1996).
- [32] B. C. Garrett, L. T. Redmon, C. W. McCurdy, and M. J. Redmon, *Phys. Rev. A* **32**, 3366 (1985).
- [33] R. Celiberto and T. N. Rescigno, *Phys. Rev. A* **47**, 1939 (1993).
- [34] A. Laricchiuta, R. Celiberto, and R. K. Janev, *Phys. Rev. A* **69**, 022706 (2004).
- [35] C. Amiot and O. Dulieu, *J. Chem. Phys.* **117**, 5155 (2002).
- [36] J. A. Coxon and P. G. Hajigeorgiou, *J. Chem. Phys.* **132**, 094105 (2010).
- [37] R. Vexiau, N. Bouloufa, M. Aymar, J. Danzl, M. J. Mark, H. Nägerl, and O. Dulieu, *Eur. Phys. J. D* **65**, 243 (2011).
- [38] M. Foucrault, P. Millie, and J. P. Daudey, *J. Chem. Phys.* **96**, 1257 (1992).
- [39] M. Krauss and W. Stevens, *J. Chem. Phys.* **93**, 4236 (1990).
- [40] B. Busserly and M. Aubert-Frécon, *J. Chem. Phys.* **82**, 3224 (1985).
- [41] F. Vigné-Maeder, *Chem. Phys.* **85**, 139 (1984).
- [42] G. H. Jeung, F. Spiegelmann, J. P. Daudey, and J. P. Malrieu, *J. Phys. B* **16**, 2659 (1983).
- [43] M. W. Schmidt, K. K. Baldrige, J. A. Boatz, E. S. T., M. S. Gordon, J. H. Jensen, S. Koseki, N. Matsunaga, K. A. Nguyen, S. Su *et al.*, *J. Comput. Chem.* **14**, 1347 (1993).
- [44] T. Leininger, A. Nicklass, W. Kuchle, H. Stoll, M. Dolg, and A. Bergner, *Chem. Phys. Lett.* **255**, 274 (1996).
- [45] W. Florian and A. Reinhart, *Phys. Chem. Chem. Phys.* **7**, 3297 (2005).
- [46] J. P. Woerdman, *J. Chem. Phys.* **75**, 5577 (1981).
- [47] J. Bai *et al.*, *Phys. Rev. A* **83**, 032514 (2011).
- [48] A. A. Radtsig and B. M. Smirnov, *Handbook of Atomic and Molecular Physics* (Atomizdat, Moscow, 1980).
- [49] A. Laricchiuta, R. Celiberto, and M. Capitelli, *Chem. Phys. Lett.* **329**, 526 (2000).
- [50] State-to-state cross sections are available upon request.